Journal Pre-proofs

NON-LOCAL VOLUMETRIC APPROACH TO ANALYSIS DEFECT'S SHAPE INFLUENCE ON SPECIMENS DURABILITY SUBJECTED TO BENDING AND TORSION

Zbigniew Marciniak, Ricardo Branco, Rui F. Martins, Wojciech Macek, Dariusz Rozumek

PII: S0142-1123(22)00567-9
DOI: https://doi.org/10.1016/j.ijfatigue.2022.107317
Reference: JIJF 107317

To appear in: *International Journal of Fatigue*

Received Date: 16 April 2022
Revised Date: 12 August 2022
Accepted Date: 3 October 2022

Please cite this article as: Marciniak, Z., Branco, R., Martins, R.F., Macek, W., Rozumek, D., NON-LOCAL VOLUMETRIC APPROACH TO ANALYSIS DEFECT'S SHAPE INFLUENCE ON SPECIMENS DURABILITY SUBJECTED TO BENDING AND TORSION, *International Journal of Fatigue* (2022), doi: https://doi.org/10.1016/j.ijfatigue.2022.107317

Submitted to International Journal of Fatigue
VSI: Fatigue – ICSI2021
August 2022

NON-LOCAL VOLUMETRIC APPROACH TO ANALYSIS DEFECT'S SHAPE INFLUENCE ON SPECIMENS DURABILITY SUBJECTED TO BENDING AND TORSION

Zbigniew Marciniak[a]*, Ricardo Branco[b], Rui F. Martins[c], Wojciech Macek[d], Dariusz Rozumek[a],

[a]*Opole University of Technology, Department of Mechanics and Machine Design, Mikołajczyka 5, 45-271 Opole, Poland*

[b]*CEMMPRE, Department of Mechanical Engineering, University of Coimbra, Rua Luís Reis Santos, Pinhal de Marrocos, 3030-788 Coimbra, Portugal*

[c]*UNIDEMI, Department of Mechanical and Industrial Engineering, Nova School of Science and Technology, Universidade NOVA de Lisboa, Campus de Caparica, 2829-516 Caparica, Portugal*

[d]*Gdańsk University of Technology, Faculty of Mechanical Engineering and Ship Technology, 11/12 Gabriela Narutowicza, Gdańsk, 80-233, Poland*

* Corresponding author: z.marciniak@po.edu.pl

Abstract

The influence of defect features on fatigue behaviour is a complex trivial issue. Although the important advances over the last decades, the dialectical relationship between the defect orientation and durability is not clearly understood. The paper aims at studying the influence of the orientation of elliptical defects on the durability of samples made of C45 steel. Three types of samples with elliptical defects were subjected to cyclic bending and torsion (R = -1) in the form of a one-sided notch oriented at various angles, namely 45, 60 and 90 degrees. The stress analysis was performed using local and non-local methods in order to determine an equivalent stress amplitude. The stress fields surrounding the defects were evaluated via three-dimensional numerical models. Then, the results were compared with the results obtained for smooth samples. The results show that the defect orientation has a higher effect under bending loading than under torsion and that the defects oriented perpendicularly to the longitudinal axis of the specimen are more detrimental.

Keywords: Bending, torsion, non-local method, defects, fatigue.

Nomenclature

A_5 - permanent elongation for a specimen with the ratio of a gage length to a diameter of a specimen equal to 5

E - Young's modulus

K_t - theoretical stress concentration factor

B - bending moment

T - torsion moment

n' - cyclic strain hardening exponent

N - number of cycles

R - load ratio

V - volume

σ - normal stress

τ - shear stress

ν - Poisson‘s ratio

σ_y - yield stress

σ_{UTS} - ultimate stress

Abbreviations

EDM - electrical discharge machining

FEM - finite elements method

FE - finite elements

Subscripts and others

b - bending

cr - critical

eq - equivalent

i, j - direction x, y, z

t - torsion

p - principal

s - smooth

1. Introduction

The failure of metallic components subjected to cyclic loading is often associated with the presence of defects [1,2]. Defects, in this context, can be divided into [3]: *imperfections* (e.g. porosities, inclusions, microvoids, cavities, etc.); and *micro-geometric flaws* (e.g. dents, scratches, corrosion pits, etc.). These material imperfections [5-6], despite the constant improvement of manufacturing routes, are naturally present in engineering applications and have significant implications for their durability. Therefore, the development of reliable fatigue

life prediction models requires a direct correlation between defect features (e.g. type, size, shape, orientation, location, etc.) and durability [6-7].

Although the detrimental effect of defects on fatigue strength is clear, the mechanisms behind this dialectical relationship are not fully understood. Roy et al. [8] studied the effect of natural and artificially introduced surface imperfections on the high-cycle fatigue behavior of A356-T6 aluminium alloy subjected to tension, torsion, and combined tension-torsion. The maximum size of the natural defects was about 450 - 700 μm, while the natural defects on the surface were in the range of 0 - 100 μm and the maximum internal defects reached 300 - 500 μm. An interesting outcome was that the critical defect size was found to be 400 ± 100 μm for both artificial and natural defects under the three loading scenarios.

Mu et al. [9] also addressed the effect of artificially introduced defects on fatigue life of AS7G06 aluminium alloy under cyclic tension considering both symmetrical (R = -1) and asymmetrical (R = 0.1) loading cases. The authors concluded that the fatigue strength was significantly reduced for defects with sizes greater than 300 μm, which was in the same order of magnitude of the grain size. On the contrary, natural casting defects smaller than 100 μm did not affect the fatigue performance in the tested range. Furthermore, it was also found that artificial defects with sizes in the interval 400 - 900 μm led to much lower maximum allowable stress levels.

Gonzalez et al. [10] studied the correlation between fatigue strength and defect size in A319-T7 aluminium alloys subjected to tension-compression at room temperature and 130°C. It was observed that the fatigue cracks were originated in pores near the outer surface. In addition, both single crack initiation and multiple crack initiation phenomena were observed. The former

phenomenon occurred at higher nominal stress levels, while the latter occurred at lower nominal stress levels. The results showed a reduction in fatigue limit by 10% at the higher temperature. In addition, it was distinguished a tendency for the reduction of fatigue life with the increase in the size of critical defect.

Toribio et al. [11] anlaysed the role of surface defects on fatigue crack initiation in pearlitic steel manufactured by two technological processes, namely hot rolled (not cold drawn) and commercially prestressed (cold drawn and stress relieved). The authors concluded that the manufacturing route can significantly affect the population of defects. It was found that the cold drawn steel exhibited seven times less micro-defects than the hot rolled steel. In a similar way, the fatigue performance was also quite influenced by the manufacturing route. Although the failure occurred from surface defects for both steels, fatigue crack initiation lives were quite higher for the cold drawn steel than for the hot rolled steel.

Gao et al. [12] studied the fatigue strength of railway axles made of low-carbon steel with different surface damage defects introduced artificially, namely craters through electronic discharge machine, indentation via compressing balls, and foreign object damage by tungsten steel balls or cubes. The first type of defects was less dangerous than the defects introduced by the other two methods. In another interesting study, Gao et al. [13] addressed the effect of surface defects created by impact damage of flying objects on fatigue resistance of high-speed railway axes. It was found that the fatigue performance it not only affected by the damage depth but also by the damage orientation and the damage shape.

The influence of a defect on fatigue life can be accounted for using different methods. Linear elastic fracture mechanics is a classical approach to analyse long cracks with homogeneous

stress fields and not affected by local plasticity. Nevertheless, these limitations make it unsuitable for short cracks [14]. Another alternative approach is the so-called √area parameter, introduced by Murakami, which corresponds to the square root of the surface of the defect projected into the direction perpendicular to the maximum stress [15]. Based on experimental evidence, it was demonstrated that the √area parameter and maximum stress intensity factor can be linearly correlated, and that the fatigue crack growth threshold is a function of the Vickers hardness. Its main limitation is the inability to describe the stress state, hindering the application to general multiaxial loading [6].

The Theory of Critical Distances is one of the most versatile tools to correlate the fatigue strength with a critical distance from an intrinsic defect size [16]. The influence of the defect is accounted for through the calculation of an equivalent stress which can be computed in different ways, namely the point method, line method, area method, or volume method [17]. Gradient-based approaches are also sophisticated tools to estimate the impact of a defect on fatigue behaviour [18]. In this case, the equivalent stress is calculated by introducing weight functions sensitive to the stress gradient in the vicinity of the defect. In recent years, advanced probabilistic fatigue methods able to capture the effect defects on fatigue behaviour have also been successfully implemented [19-20]. More recently, these methods, combined with other advanced approaches, such as the weakest link theory or the energy field intensity approach, were successfully used to account for notch and size effects [21-22]. A comprehensive review on notch and size effects can found in the paper by Zhu et al. [23].

Although there is a clear relationship between defect size and fatigue life, the influence of defect orientation on fatigue behaviour is not clearly understood. To the best of the authors' knowledge, there are no studies addressing this topic. Thus, this paper aims to study the effect

of the defect orientation on fatigue durability in C45 structural steel under cyclic bending and torsion (R = -1). Elliptical defects with the form of a one-sided notch and placed at three different orientations (45^o, 60^o, and 90^o) with respect to the main axis of the specimen are studied. The stress fields surrounding the defect are computed using three-dimensional numerical models. The stress analysis is conducted using both local and non-local approaches.

2. Material and methods

Structural steel C45, commonly used for medium-loaded and wear-resistant machine parts, was selected for the fatigue tests. The chemical composition and mechanical properties are presented in Tables 1 and 2. Its microstructure, examined via optical microscopy is presented on Fig. 1. As can be seen, the material was characterized by a ferritic-pearlitic structure, and the percentage of perlite was 52%. The grains of perlite and ferrite are evenly distributed in the structure. The grain size is not very diversified and the average grain size is 6.44 μm.

Figure. 1.

Table 1.

Table 2.

Four types of cylindrical samples with a diameter of 10 mm, were tested: (1) smooth (without a defect); (2) with a defect of length 3.5 mm at an angle of 90°(Fig. 2a); (3) with a defect of length 4 mm at an angle of 60° (Fig. 2b), and (4) with a defect of length 4.9 mm at an angle of 45° (Fig. 2c). The specimens were cut from a drawn bar with a diameter of 20 mm and then subjected to the normalization process. The defects were made employing wire electrical discharge machining (EDM) with a diameter of 0.64 mm and a depth of 0.32 mm. The defect

system was designed in such a way that the Murakami parameter (√area) was the same for all defect samples for bending loading.

Figure. 2.

The quality of the defects was checked on the Alicona Infinite G4 surface topography stand, where the area of the defect was scanned, and then, using the MountainsMap software, surface roughness and defect depth analyzes were carried out to eliminate samples with deviating geometric parameters [24]. Fig. 3 shows typical examples of the analyses of defects conducted with the optical microscope for three different orientations, namely 90°, 60°, and 45°. The pseudo-colours represent the values of the distance measured from the deepest point of the defect surface. As can be seen in the figure 3, the measured values meet the geometrical definitions.

Figure. 3.

The MZGS-100Ph fatigue machine [25,26] was used to perform the experimental tests. The samples were subjected to cyclic bending and torsion. The tests were carried out in the high-cycle fatigue regime, under constant-amplitude load, for a load ratio (R) equal to -1, and a cyclic frequency of 27.5 Hz. The bending moments and the torsion moments varied from 12.5 to 27.5 N·m and 30 to 45 N·m, respectively. For each defect geometry, at least two specimens were tested. The tests were completed when the stiffness of the samples have decreased by 20%.

The stress analysis at the defect region was performed using a three-dimensional finite-element model. The mesh was developed in a unstructured manner employing 4-node tetrahedral finite

elements (see Fig. 4). In order to better characterise the stress fields at the geometric discontinuity, a ultra-refined patter was used in that region (see Fig. 4(b)). In remote positions, to alleviate the computation effort, the mesh density was reduced. The numbers of elements and the numbers of nodes for each defect configuration are listed in Table 3.

As far as the boundary conditions are concerned, the ends of the specimen were connected to two prismatic bodies to simulate the gripping system of the testing machine. One of them was fixed while the other was used to apply the loading cases (bending moment or torsion moment) considered in the experimental program. The material was defined as continuous, homogeneous, and isotropic. The simulations were carried out assuming a linear-elastic behaviour via the generalised Hooke's law. The material constants of the tested material are summarised in Table 2.

Figure. 4.

Table 3.

3. Fatigue results

The tests were carried out in a way that made it possible to determine the lowest possible load level for each type of sample and load (bending or torsion). As referred to above the tests were completed when the stiffness of the samples has decreased by 20%. The research was carried out in the high-cycle fatigue regime (HCF) with R = -1. The results of the fatigue tests, in terms of bending moment versus number of cycles to failure and torsion moment versus number of cycles to failure are shown in Fig. 5(a) and Fig. 5(b), respectively.

As can be seen in the figure, the fatigue performance of the specimens with elliptical defects is governed by the defect orientation, either under bending or under torsion. For instance, by comparing the cases of the 45º and 60º orientations, which were subjected to the loading levels, we can conclude that the former have higher lives under bending but lower lives under torsion and vice-versa.

The maximum stress at the defect region was accounted for using the theoretical stress concentration factors. The theoretical stress concentration factor were determined using finite element models (Femap software) developed for the different geometrical discontinuities (see Fig. 4). The maximum stress for the calculation of the theoretical stress concentration was taken from the middle of the sample length in the case of the smooth samples, while in the case of samples with defect it was taken from the bottom of the defect. The values were equal to 2.6, 2.34 and 2.04 for bending (determined from Eq.(1)), respectively, for samples with a defect at the angle of 90, 60 and 45 degrees, and approximately 1.7 for torsion (determined from Eq. (2)).

$$K_{tb} = \frac{\sigma_{max}}{\sigma_s} \qquad (1)$$

$$K_{tt} = \frac{\tau_{max}}{\tau_s} \qquad (2)$$

The typical stress fields obtained in the simulations for bending and for torsion near the notch region are shown in Fig. 6 and Fig. 7, respectively.

Figure 5

Figure. 6

As can be seen in Fig. 6 and Fig. 7, irrespective of the loading scenario, the maximum values are located at the deepest point of the geometric discontinuity, i.e. in the center of the notch. On

the contrary, as we approach to the notch boundaries, the stress values decrease. Moreover, we can also conclude that the stress fields are symmetrical with respect to the main axes of the defect. It is also clear that the defect orientation, for a fixed bending moment or torsion moment, leads to different values of maximum stress. The analysis of Fig 6(a) and Fig. 6(b) whose simulations were computed for the same value of bending moment shows that the maximum stress values are different: the maximum value is higher for the defect at angle of 60º than for the defect at an angle of 45º.

Figure. 7.

The relationship between the stress values calculated on the basis of the theoretical notch factors and the fatigue life for bending and torsion are exhibited in Fig. 8 (a) and Fig. 8(b), respectively. As can be seen in the figures, the stress values determined by this method and the related S-N diagrams indicate significant differences, especially under bending, in the values for smooth samples, despite similar durability, which may cause erroneous interpretations in the design. Therefore, more advanced approaches are recommended to alleviate this shortcoming

Figure. 8.

4. Non-local method approach

In this section, the obtained test results were analyzed using non-local, volumetric fatigue calculation methods. For this purpose, the results of the numerical simulations were used to determine the volume in which the stress values are above the limit stress. This volume will hereinafter be referred to as the critical stress volume and is given by:

$$\sigma_{eq} = \frac{1}{V_{cr}} \int_{V_{cr}} f(\sigma_{ij}) dV \qquad (3)$$

where σ_{eq} is the equivalent stress, V_{cr} is the critical stress volume, and $f(\sigma_{ij})$ is the stress components used to calculate the equivalent stress. For the calculation of the equivalent stress, the critical stress was selected as the reference level, which corresponds to the lowest value of the stress amplitude at which failure occurred in the tests of smooth samples.

Three different averaging criteria were considered: the Huber-Mises stress, represented by $\sigma_{HM,ave}$ (see Eq. (4)), which accounts for the average stress using the entire stress tensor; the first principal stress, represented by $\sigma_{1,ave}$ ((see Eq. (5)), which computes the average stress from the first principal stress field; and the normal stress (along x-axis), represented by $\sigma_{x,ave}$, which calculates the average stress from the normal stress distribution in the vicinity of the defect region.

$$\sigma_{HM} = \sqrt{\frac{1}{2}\left[(\sigma_x - \sigma_y)^2 + (\sigma_y - \sigma_z)^2 + (\sigma_z - \sigma_x)^2\right] + 3\left(\tau_{xy}{}^2 + \tau_{yz}{}^2 + \tau_{zx}{}^2\right)} \qquad (4)$$

$$\sigma_p{}^3 - (\sigma_x + \sigma_y + \sigma_z)\sigma_p{}^2 + \left(\sigma_x\sigma_y + \sigma_x\sigma_z + \sigma_z\sigma_y - \tau_{xy}{}^2 - \tau_{yz}{}^2 - \tau_{zx}{}^2\right)\sigma_p - (\sigma_x\sigma_y\sigma_z + 2\tau_{xy}\tau_{yz}\tau_{zx} - \sigma_x\tau_{yz}{}^2 - \sigma_y\tau_{xz}{}^2 - \sigma_z\tau_{yx}{}^2) = 0 \qquad (5)$$

The values of particular stresses and the volumes of each finite element are taken from the software, and then depending on the level of the so-called critical stress are summed the stress and volume products of particular finite elements. If the stress value in a finite element is lower than the critical stress, then such elements are omitted. Finally, the sum of the products obtained is divided by the total volume of the involved elements.

The determined volumes for the different loading cases differed depending on the selected criterion (see Table 4). As can be seen, the smallest volume of critical stresses was found for the equivalent stress criterion according to the Huber-Mises hypothesis ($\sigma_{HM,ave}$), and the largest for the first principal stress ($\sigma_{1,ave}$). In addition, despite the values of the critical stress volumes

are different, the three criteria exhibit the same trends. Furthermore, it is also clear that the values vary with the defect orientation and the loading type.

Regarding the defect orientation, by comparing the cases of 45º and 60º, which were subjected to the same loading level, we can conclude that the critical stress volumes are smaller for 45º than for 60º, either for bending or torsion. The effect of loading type can be inferred by comparing any of the three defect orientations. For instance, for a defect at an angle of 60º, the values for torsion are greater than for bending.

Table 4.

Table 5.

Figure. 9.

Figure. 10.

Figures 9 and 10 plot the calculated average stresses against the number of cycles to failure for the bending cases and the torsion cases, respectively. By analyzing the results obtained for the criteria selected above(Figs. 9-10), a significant decrease in the averaged stresses related to the stress values obtained from the FEM calculations can be observed, e.g. for the sample with a defect at an angle of 60°, the stress decreased by 120 MPa for a sample with a defect at an angle of 45° the stress decreased by 70 MPa and for a defect at an angle of 90°,the stress decreased by 50 MPa.

The results obtained by the non-local volumetric method approximate the amplitude values of the samples with defects to the results of the smooth samples, which is an interesting outcome and demonstrates the design capabilities of this advanced approach. In a practical point of view, the experiments also indicate that the defect configuration perpendicular to the longitudinal axis of the sample is the most harmful in terms fatigue performance.

In the case of torsion, the orientation of the elliptical defects has a smaller effect on the fatigue life. However, the application of the Huber-Mises method shows the best results.

Moreover, the analysis for the experimental cases in which specimens have not been damaged showed that the critical volume was equal to 0. Thus, the non-local volumetric method can provide a new tool for engineers and significantly reduce the time and money of experimental research.

5. Concluding remarks

This paper studied the influence of the orientation of elliptical defects on the durability of samples made of C45 steel subjected to bending and torsion. Specimens with elliptical defects with three orientations (45º, 60º, and 90º) with respect to the main axis of the specimen were studied. The stress fields in the vicinity of the geometric discontinuity were computed using three-dimensional numerical models. The stress analysis was conducted using local and non-local criteria. The following conclusions can be drawn:

- The experimental tests show that the smallest bending moment necessary to damage the sample occurs in the sample with an elliptical defect oriented perpendicular to the longitudinal axis of the specimen;
- The defect orientation has a higher effect on fatigue life under bending than under torsion, and defects oriented at an angle of 90º are more detrimental to fatigue performance;

- Under bending, the specimens with a defect oriented at a 60º required much higher stress levels to fail than the specimens with defects oriented at a 45º;
- Determination of equivalent stress using the non-local volumetric method showed that the values of these stresses came much closer to the stress values for smooth samples;
- The analysis demonstrated that the non-local volumetric method can provide a new tool for engineers in terms of fatigue design. Moreover, it significantly reduces the time and money associated with the experimental program.

Acknowledgement

This research is sponsored by FEDER funds through the program COMPETE – Programa Operacional Factores de Competitividade – and by national funds through FCT – Fundação para a Ciência e a Tecnologia – under the projects UIDB/00285/2020 and UIDB/00667/2020.

Author Contributions

Z. Marciniak: Conceptualization, Methodology, Investigation, Writing - Original Draft, Writing - Review & Editing, Visualization, **R. Branco**: Writing - Original Draft, Writing - Review & Editing, Visualization, **R. F. Martins**: Writing - Original Draft, Writing - Review & Editing, **W. Macek**: Writing - Original Draft, Writing - Review & Editing, **D. Rozumek**: Writing - Original Draft, Writing - Review & Editing

References:

[1]. R.M. Nejad, F. Berto. Fatigue crack growth of a railway wheel steel and fatigue life prediction under spectrum loading conditions. Int. J. of Fatigue 157 (2022), 106722.

[2]. H. Xin, M. Veljkovic, J.A.F.O. Correia, F. Berto. Ductile fracture locus identification using mesoscale critical equivalent plastic strain. Fatigue and Fracture of Engineering Materials and Structures 44 (2021), 1292-1304.

[3]. U. Zerbst, C. Klinger. Material defects as cause for the fatigue failure of metallic components. Int. J. of Fatigue 127 (2019), 312-323.

[4]. Macek W, Martins RF, Branco R, Marciniak Z, Szala M, Wroński S. Fatigue fracture morphology of AISI H13 steel obtained by additive manufacturing. International Journal of Fracture 2022:1–20. https://doi.org/10.1007/S10704-022-00615-5.

[5]. Macek W, Branco R, Costa JD, Trembacz J. Fracture Surface Behavior of 34CrNiMo6 High-Strength Steel Bars with Blind Holes under Bending-Torsion Fatigue. Materials 2022, Vol 15, Page 80 2021;15:80. https://doi.org/10.3390/MA15010080.

[6]. L. Viet-Duc, M. Franck, B. Daniel, S. Nicolas, O. Pierre (2016). Multiaxial high cycle fatigue damage mechanisms associated with the different microstructural heterogeneities of cast aluminium alloys. Materials Science and Engineering A 649, 426-440.

[7]. R. Branco, J.D. Costa, F. Berto, A. Kotousov, F.V. Antunes (2020). Fatigue crack initiation behaviour of notched 34CrNiMo6 steel bars under proportional bending-torsion loading. Int. J. of Fatigue 130, 105268.

[8]. M.J. Roy, Y. Nadot, C. Nadot-Martin, P.-G. Bardin, D.M. Maijer (2011). Multiaxial Kitagawa analysis of A356-T6. Int. J. of Fatigue; 33: 823-832.

[9]. P. Mu, Y. Nadot, C. Nadot-Martin, A. Chabod, I. Serrano-Munoz, C. Verdu (2014). Influence of casting defects on the fatigue behavior of cast aluminum AS7G06-T6. Int. J. of Fatigue 63, 97-109.

[10]. R. González, D.I. Martínez, J.A. González, J. Talamantes, S. Valtierra, R. Colás (2011). Experimental investigation for fatigue strength of a cast aluminium alloy. Int. J. of Fatigue 33, 273-278.

[11]. J. Toribio, J.-C. Matos, B. Gonzalez (2013). Role of surface defects in the initiation of fatigue cracks in pearlitic steel. 13th International Conference on Fracture, June 16-21, Beijing, China.

[12]. J.-W. Gao, G.-Z. Dai, Q.-Z. Li, M.-N. Zhang, S.-P. Zhu, J.A.F.O. Correia, G. Lesiuk, A.M.P. De Jesus. Fatigue assessment of EA4T railway axles under artificial surface damage, Int. J. of Fatigue 146 (2021) 106157.

[13]. J.-W. Gao, M.-H. Yu, D. Liao, S.-P. Zhu, J. Han, G. Lesiuk, J.A.F.O. Correia, A.M.P. De Jesus. Fatigue and damage tolerance assessment of induction hardened S38C axles under different foreign objects, Int. J. of Fatigue 149 (2021) 106276.

[14]. L. Susmel (2004). A unifying approach to estimate the high-cycle fatigue strength of notched components subjected to both uniaxial and multiaxial cyclic loadings. Fatigue and Fracture of Engineering Materials and Structures 27, 391-411.

[15]. Y. Murakami (2019). Metal fatigue: effects of small defects and nonmetallic inclusions. Second edition, Elsevier: Book.

[16]. D. Taylor (1999). Geometrical effects in fatigue: a unifying theoretical model, Int. J. of Fatigue 21, 413–420.

[17]. L. Susmel, D. Taylor (2006). A simplified approach to apply the theory of critical distances to notched components under torsional fatigue loading. Int. J. of Fatigue, 28, 417-430.

[18]. G. Qylafku, Z. Azari, N. Kadi, M. Gjonaj, G. Pluvinage (1999). Application of a new model proposal for fatigue life prediction on notches and key-seats. International Journal of Fatigue 21, 753-760.

[19]. Y. Ai, S.P. Zhu, D. Liao, J.A.F.O. Correia, C. Souto, A.M.P. De Jesus, B. Keshtegar (2022). Probabilistic modeling of fatigue life distribution and size effect of components with random defects. International Journal of Fatigue 126, 165-173.

[20]. L. Patriarca, S. Beretta, S. Foletti, A. Riva, S. Parodi (2020). A probabilistic framework to define the design stress and acceptable defects under combined-cycle fatigue conditions. Engineering Fracture Mechanics 224, 106784.

[21]. Y.-L. Wu, S.-P. Zhu, D. Liao, J.A. F.O Correia, Q. Wang. Probabilistic fatigue modeling of notched components under size effect using modified energy field intensity approach. Mechanics of Advanced Materials and Structures, https://doi.org/ 10.1080/15376494.2021.1977437.

[22]. X.-K. Li, S.-P. Zhu, D. Liao, J.A.F.O. Correia, F. Berto, Q.n Wang. Probabilistic fatigue modelling of metallic materials under notch and size effect using the weakest link theory. International Journal of Fatigue 159 (2022) 106788.

[23]. S.-P. Zhu, Y. Ai, D. Liao, J.A. F. O. Correia, A.M. P. De Jesus, Q. Wang. Recent advances on size effect in metal fatigue under defects: a review. International Journal of Fracture 234 (2022) 21–43.

[24]. Macek W., Marciniak Z., Branco R., Rozumek D., Królczyk GM, 2021. A fractographic study exploring the fracture surface topography of S355J2 steel after pseudo-random bending-torsion fatigue tests, Measurement, 178, 109443, https://doi.org/10.1016/j.measurement.2021.109443.

[25]. Kasprzyczak L., Macha E., Marciniak Z., Energy parameter Control System of strength Machine for Material Test under cyclic bending and torsion, Mechatronic Systems and Materials IV 198, 2013, pp.489-494.

[26]. Rozumek D., Marciniak Z., The investigation of crack growth in specimens with rectangular cross-sections under out-of-phase bending and torsional loading, Int. J. of Fatigue 39 (2012), 81-87.

Submitted to International Journal of Fatigue

VSI: Fatigue – ICSI2021

August 2022

Revision 1

NON-LOCAL VOLUMETRIC APPROACH TO ANALYSIS DEFECT'S SHAPE INFLUENCE ON SPECIMENS DURABILITY SUBJECTED TO BENDING AND TORSION

Zbigniew Marciniak[a]*, Ricardo Branco[b], Rui F. Martins[c], Wojciech Macek[d], Dariusz Rozumek[a],

[a]*Opole University of Technology, Department of Mechanics and Machine Design, Mikołajczyka 5, 45-271 Opole, Poland*

[b]*CEMMPRE, Department of Mechanical Engineering, University of Coimbra, Rua Luís Reis Santos, Pinhal de Marrocos, 3030-788 Coimbra, Portugal*

[c]*UNIDEMI, Department of Mechanical and Industrial Engineering, Nova School of Science and Technology, Universidade NOVA de Lisboa, Campus de Caparica, 2829-516 Caparica, Portugal*

[d]*Gdańsk University of Technology, Faculty of Mechanical Engineering and Ship Technology, 11/12 Gabriela Narutowicza, Gdańsk, 80-233, Poland*

* Corresponding author: z.marciniak@po.edu.pl

Figures and Tables

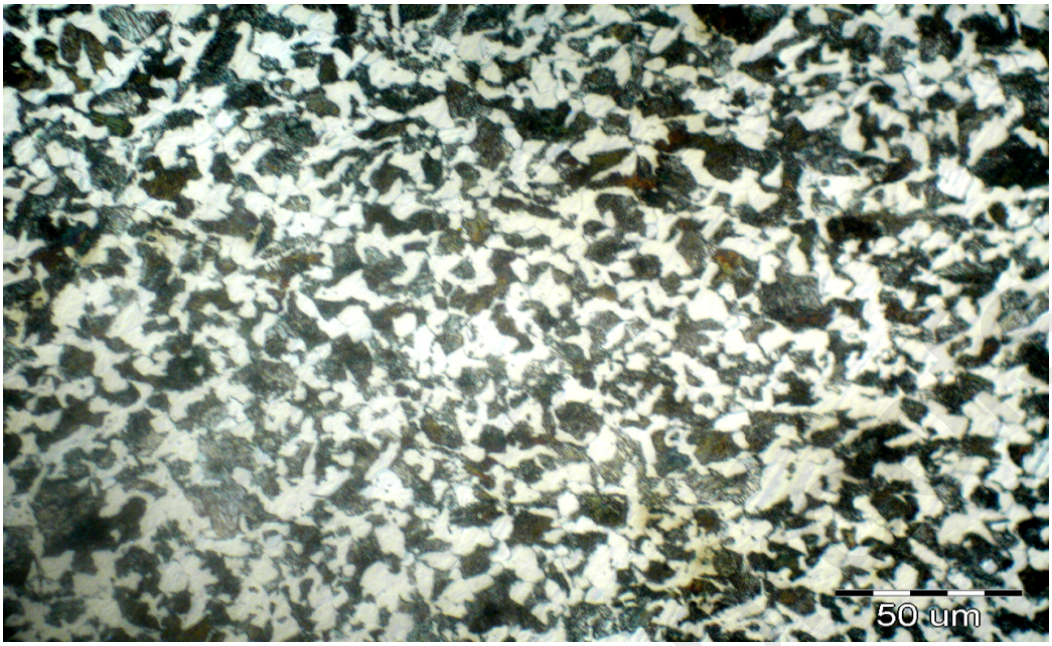

Fig. 1. Microstructure of the C45 steel.

Table 1. Chemical composition of the C45 steel.

Element	C	Si	Mn	Cr	Ni	S	P	Cu	Fe
Content %	0.42-0.5	0.17-0.37	0.5. -0.8	max. 0.3	max. 0.3	max. 0.04	max. 0.04	max. 0.3	Bal.

Table 2. Mechanical properties of the C45 steel.

σ_y MPa	σ_{UTS} MPa	ν -	E GPa	A_5 %
547	739	0.3	215	17

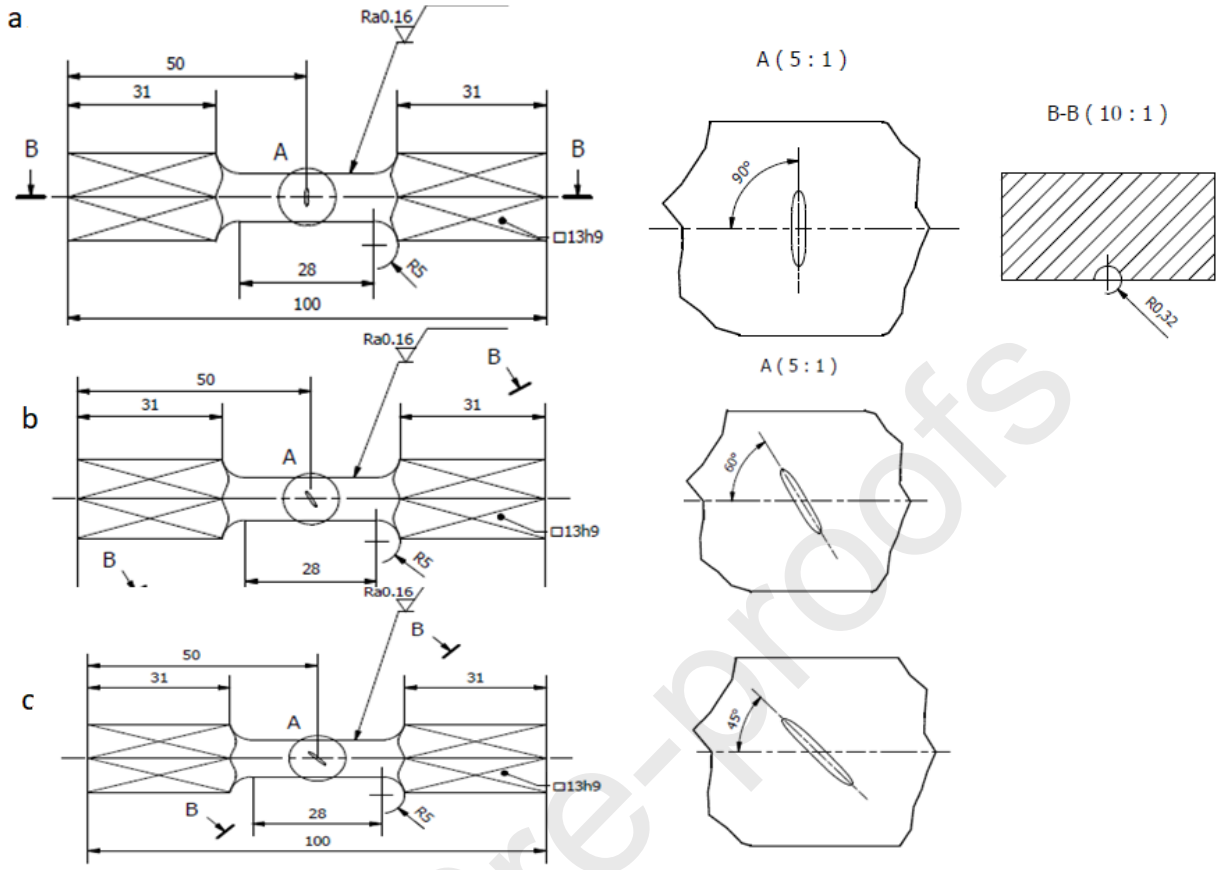

Fig. 2. Shape and dimension (in mm) of the tested specimens with the defect orientation angle (a) 90°, (b) 60°, (c) 45°.

(a)

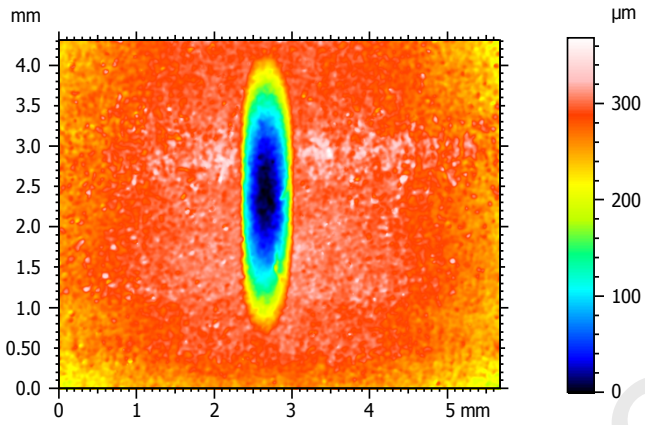

(b)

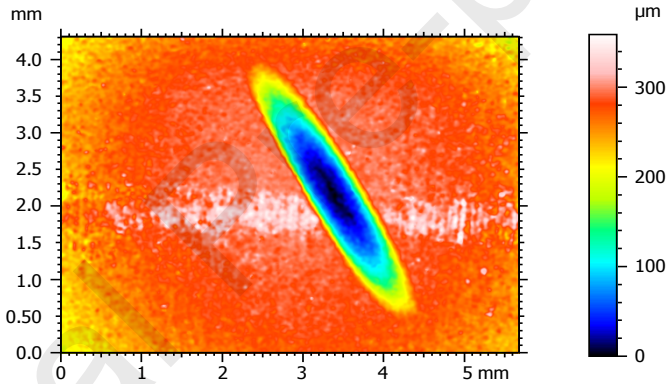

(c)

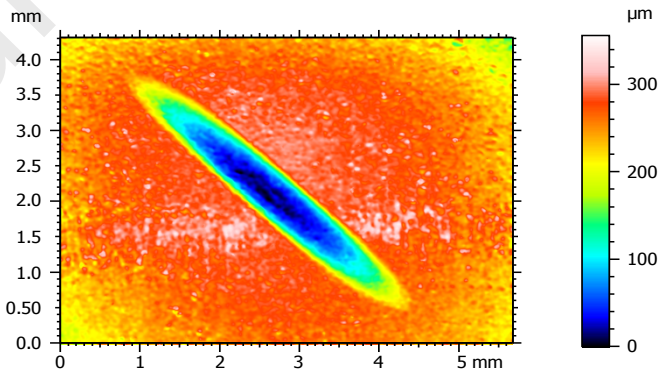

Fig. 3. Measurements results of geometrical dimensions of defects : a) 90°, b) 60°, c) 45°.

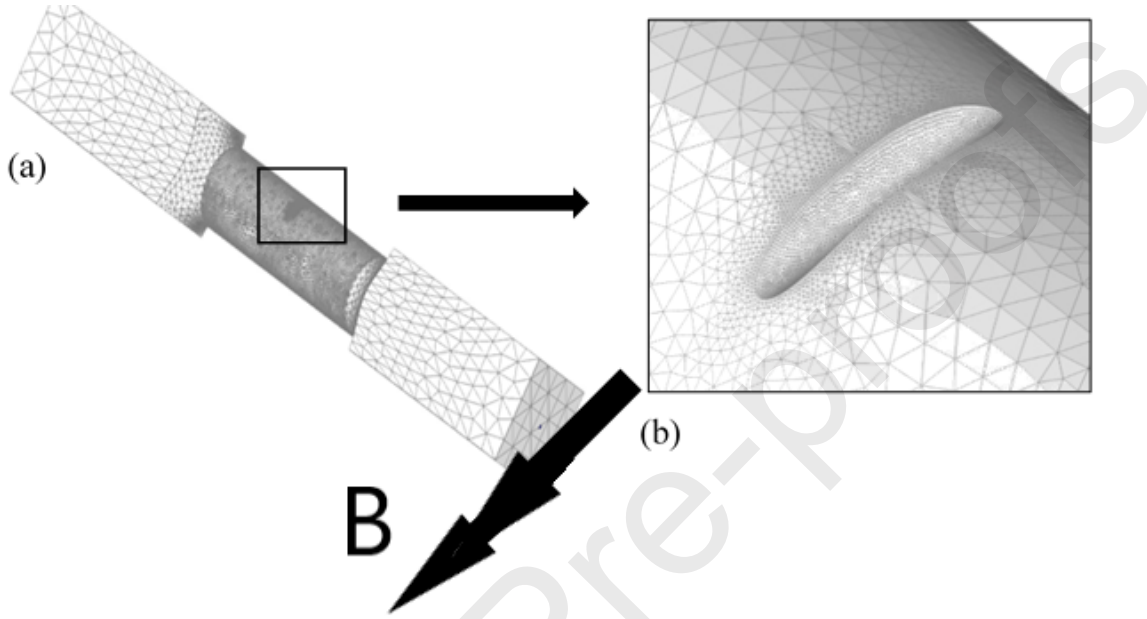

Fig. 4. (a) Finite element model of the analysed specimens with a lateral notch subjected to bending (represented by B); (b) detail of notch region for a defect with an orientation of 90º.

Table 3. FEM model properties.

Type of specimen	No. of nodes	No. of FE	The ratio of the length of the FE edge at the notch root to the notch radius
smooth	32940	21433	-
45°	220711	145588	0.07
60°	240363	158412	0.083
90°	188865	125047	0.087

(a)

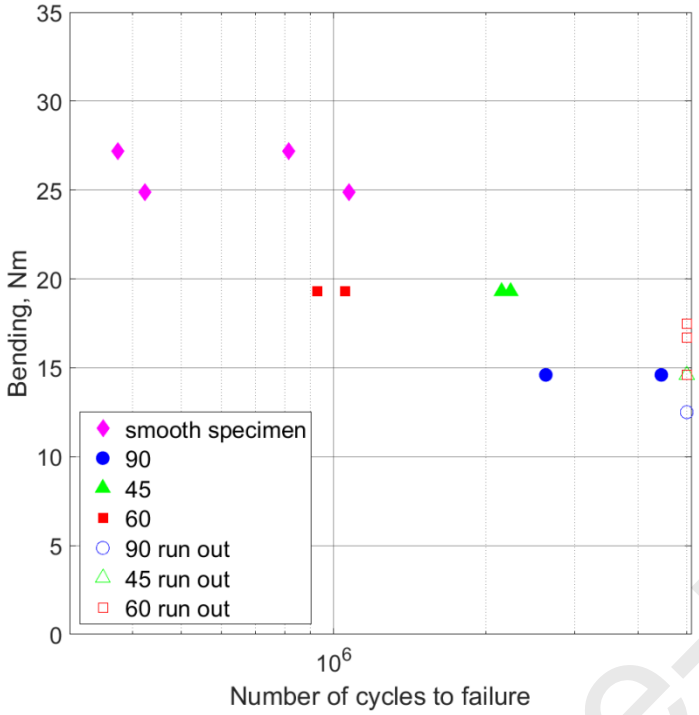

(b)

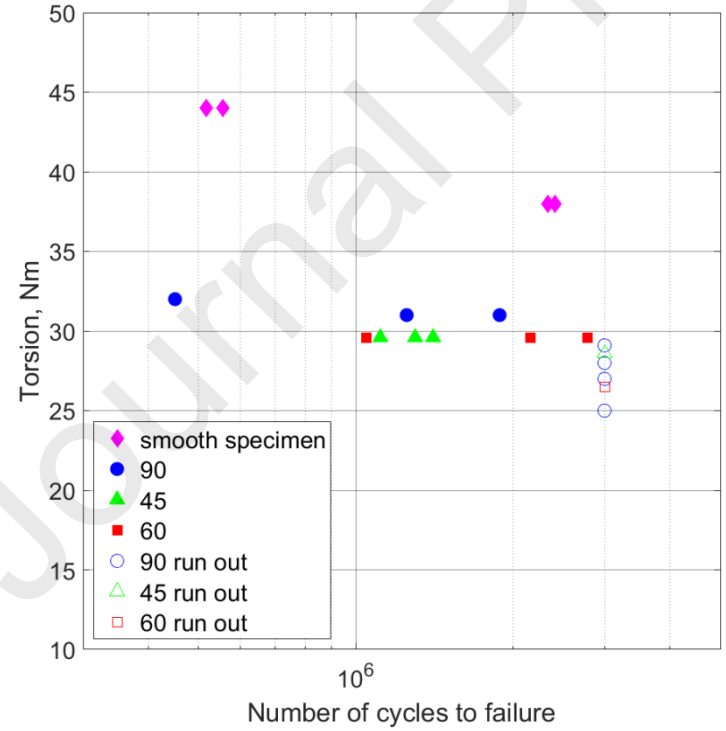

Fig. 5. Diagram of the dependence of the number cycles to failure as a function of: a) the bending moment and b) torsion moment

(a)

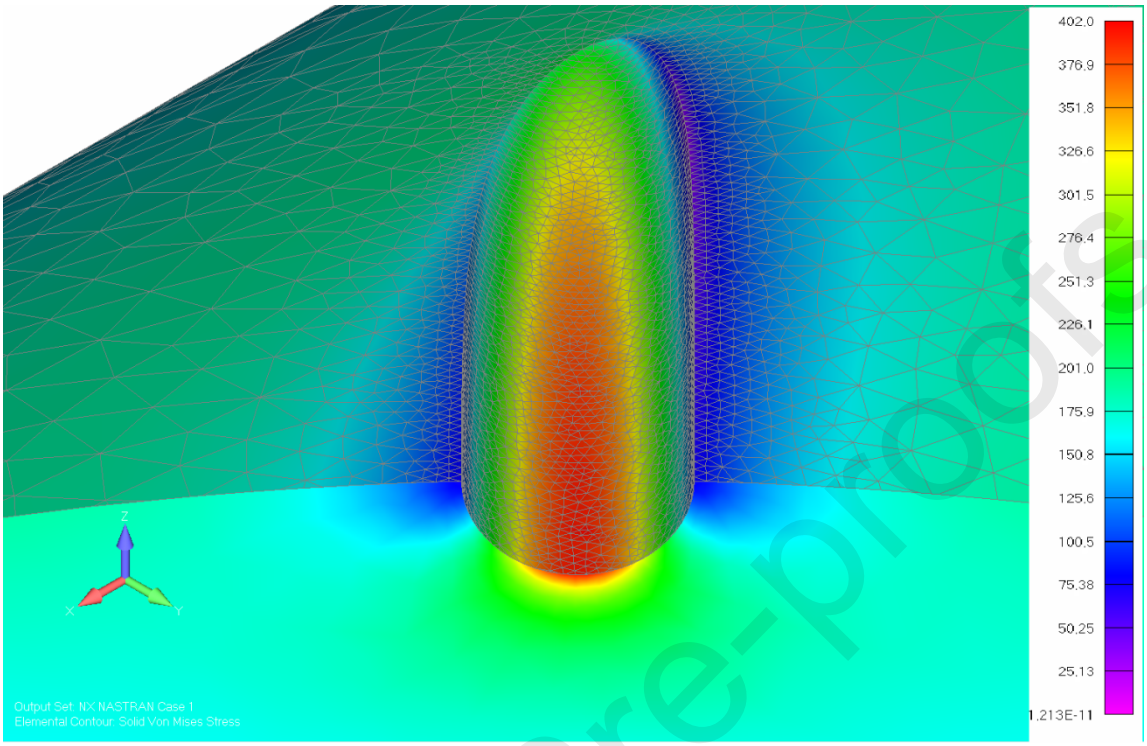

(b)

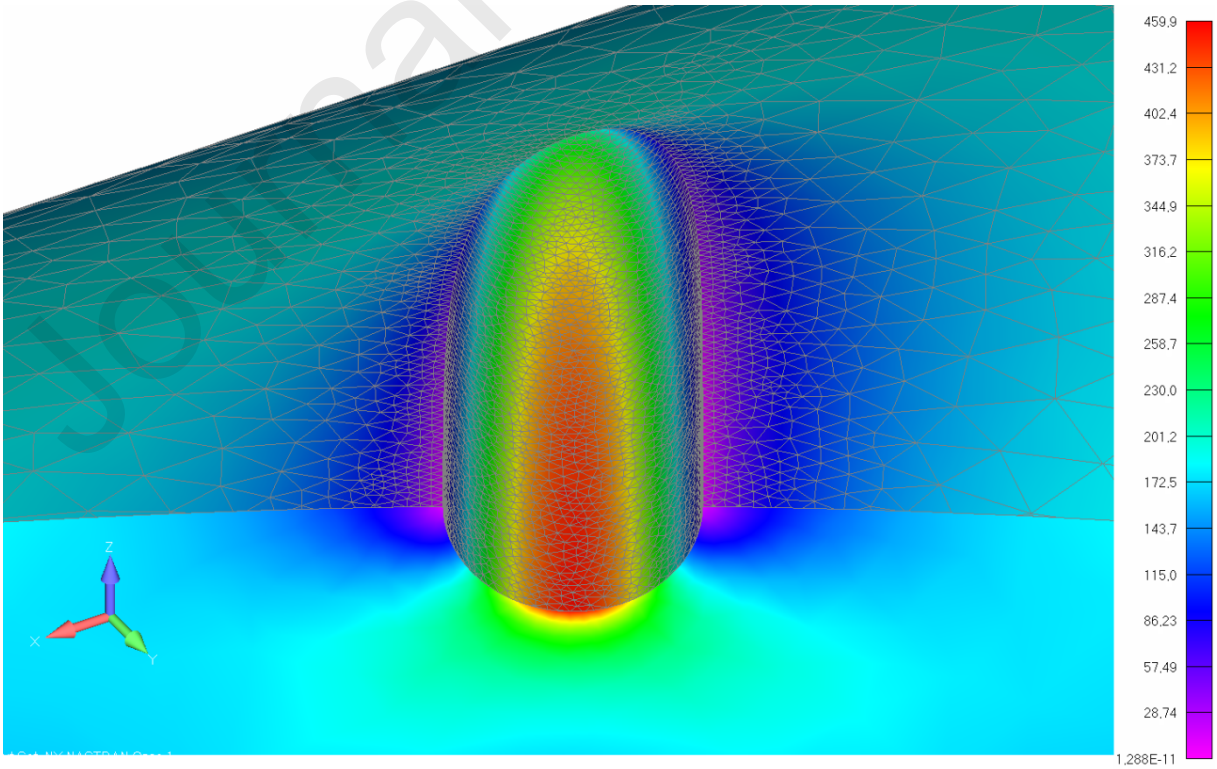

(c)

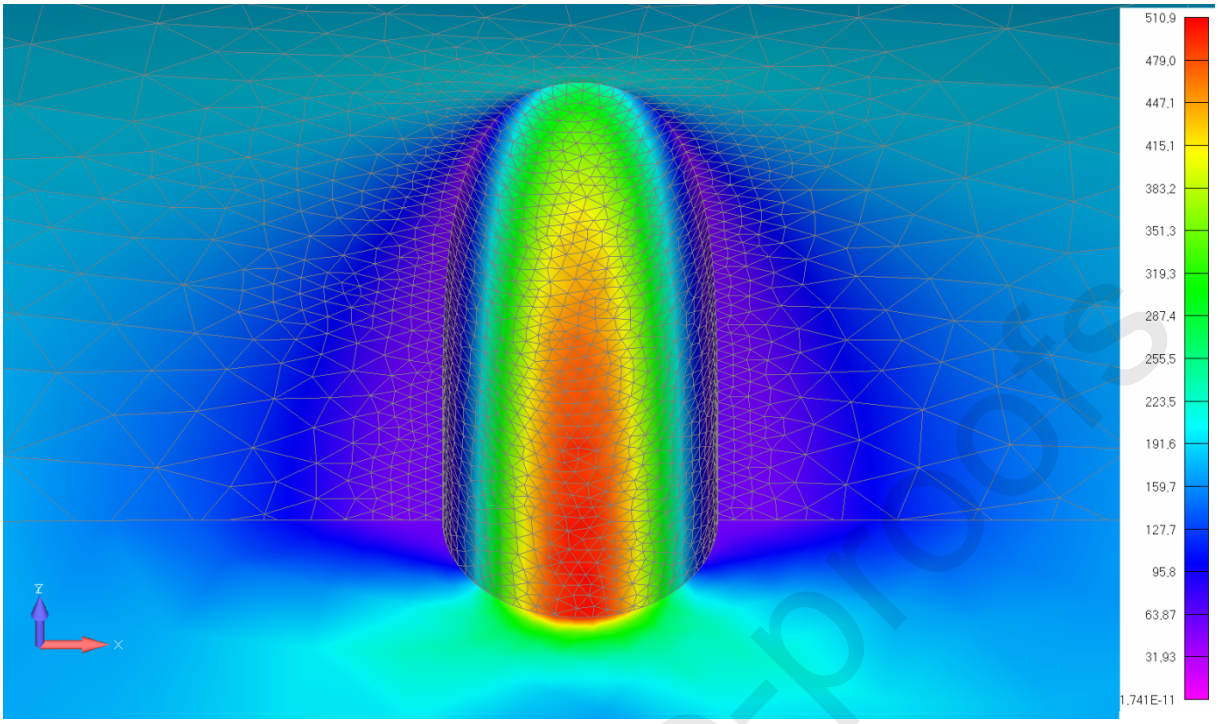

Fig. 6. Stress distribution according to the Huber-Mises hypothesis: (a) 45° for a bending moment of 19.3 N·m (b) 60° for a bending moment of 19.3 N·m, (c) 90° for a bending moment of 14.3 N·m.

(a)

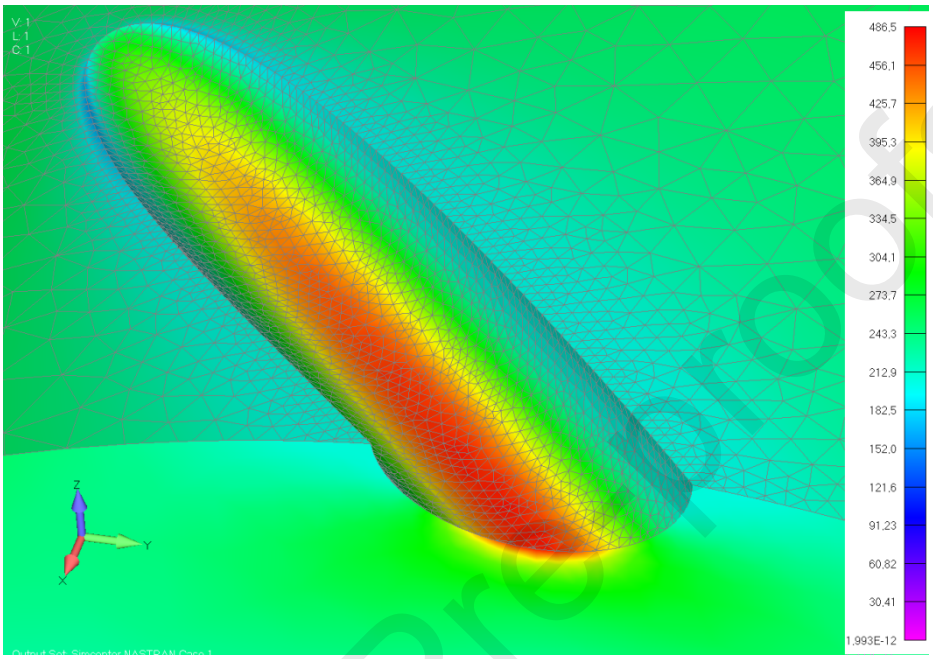

(b)

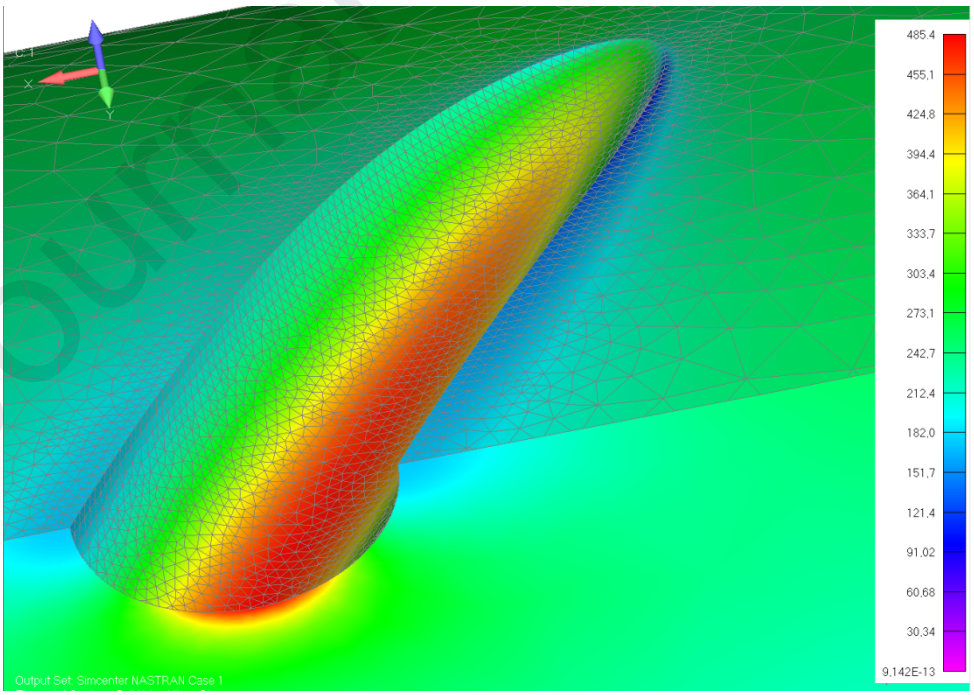

(c)

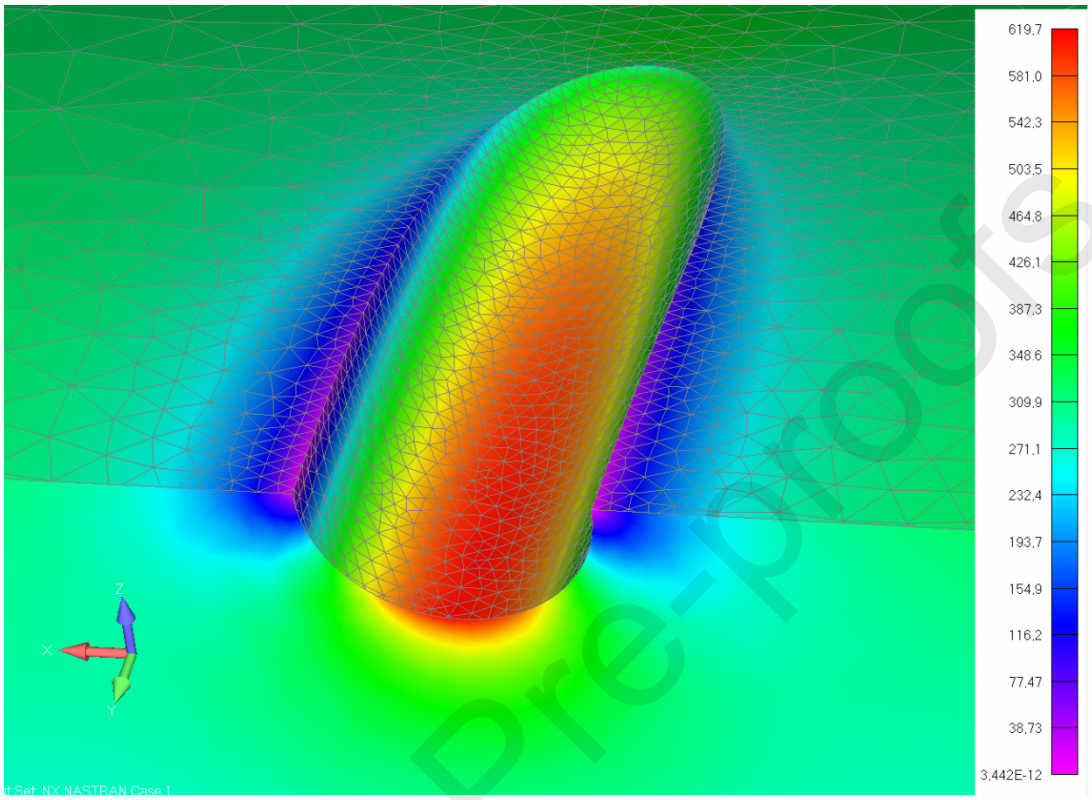

Fig. 7. Exemplary stress distribution according to the Huber-Mises hypothesis: (a) 45° for a torsion of 29.6 N·m, (b) 60° for a torsion of 29.6 N·m, (c) 90° for a torsion of 31 N·m.

(a)

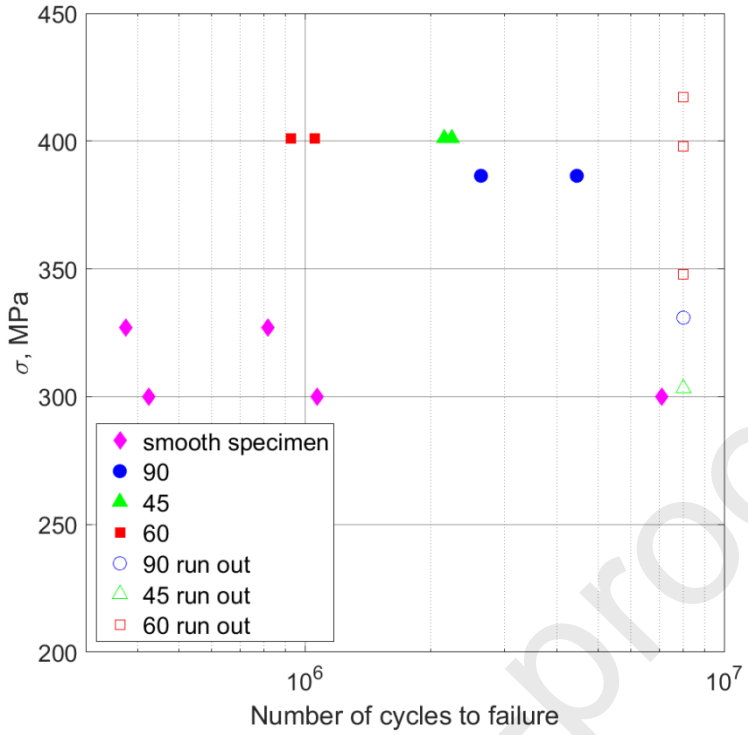

(b)

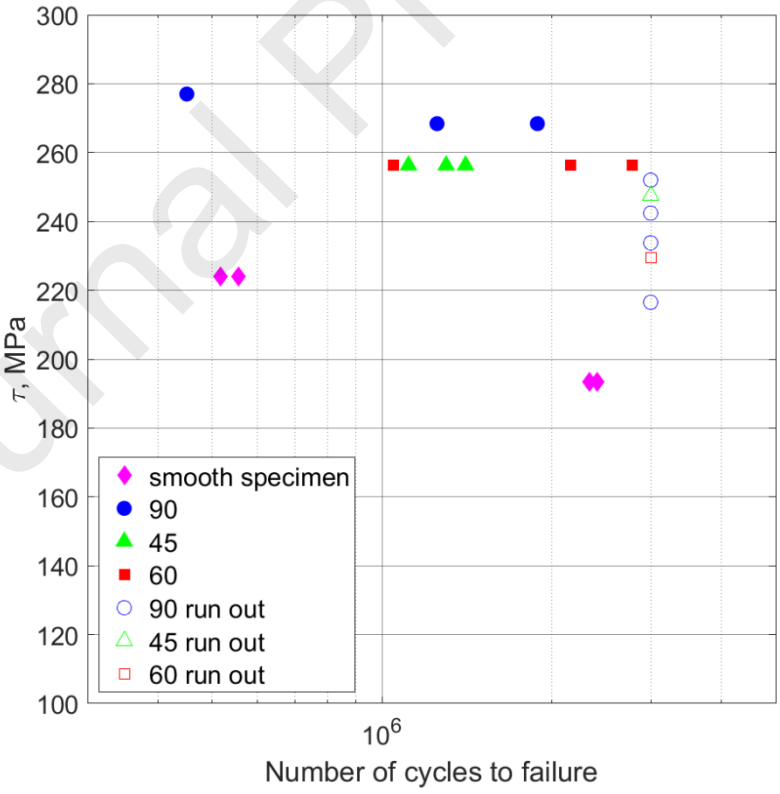

Fig. 8. S-N plot for stresses amplitudes calculated using the theoretical stress concentration notch factors: (a) bending load, (b) torsion load.

Table 4. Size of the critical volume in mm^3.

	Bending			Torsion		
	45°	60°	90°	45°	60°	90°
	19.3 N·m	19.3 N·m	14.6 N·m	29.6 N·m	29.6 N·m	31 N·m
σ_{H-M}	0.046	0.058	0.011	0.011	0.081	0.115
σ_1	0.065	0.094	0.025	0.147	0.304	0.140
σ_x	0.049	0.080	0.020	-	-	-

Table 5. Values of averaged stress in MPa corresponding to critical size volume in Table 4.

	Bending			Torsion		
	45°	60°	90°	45°	60°	90°
	19.3 N·m	19.3 N·m	14.6 N·m	29.6 N·m	29.6 N·m	31 N·m
$\sigma_{H\text{-}M}$	327.8	342	322	349.5	370.5	373.8
σ_1	329.7	345.4	334.2	288	239	224
σ_x	326.8	348	334.7	-	-	-

(a)

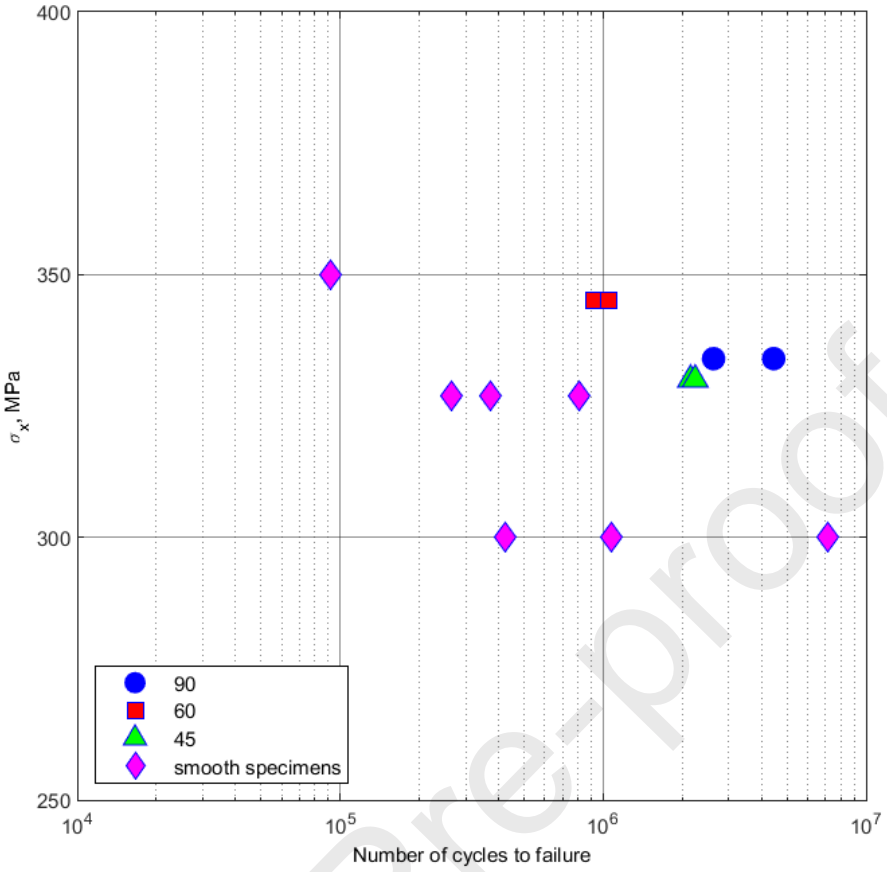

(b)

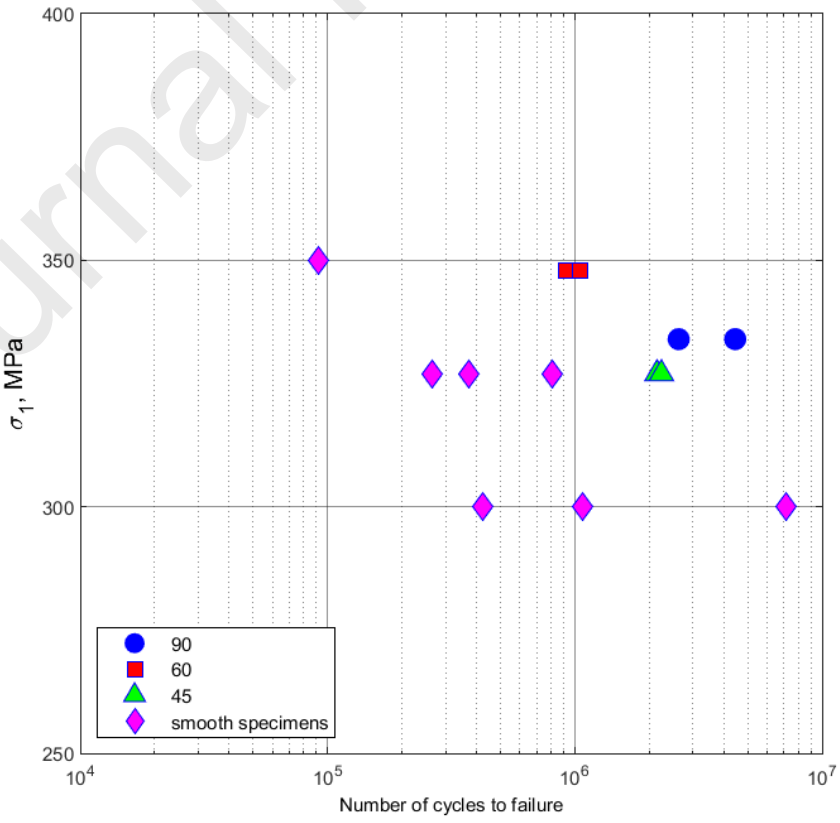

(c)

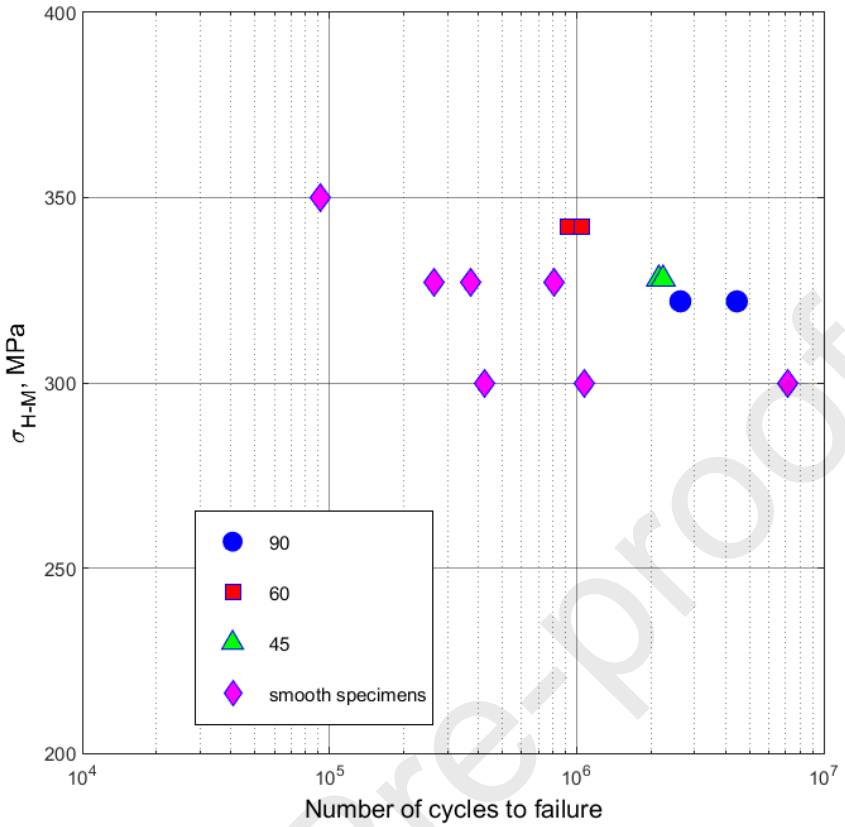

Fig. 9. S-N diagram for stresses calculated according to the different averaging criteria under bending: (a) normal stress σ_{x_ave} and (b) first principal stress σ_{1_ave}, (c) Huber-Mises $\sigma_{HM,ave}$.

(a)

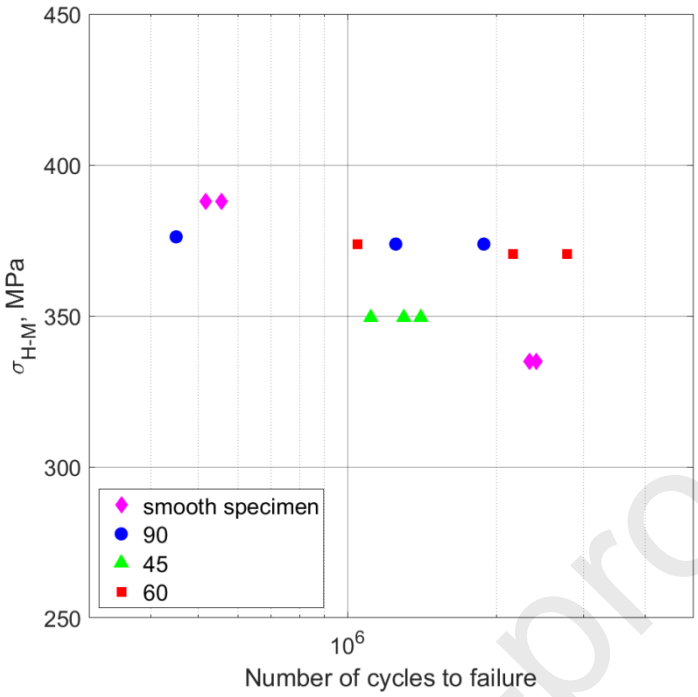

(b)

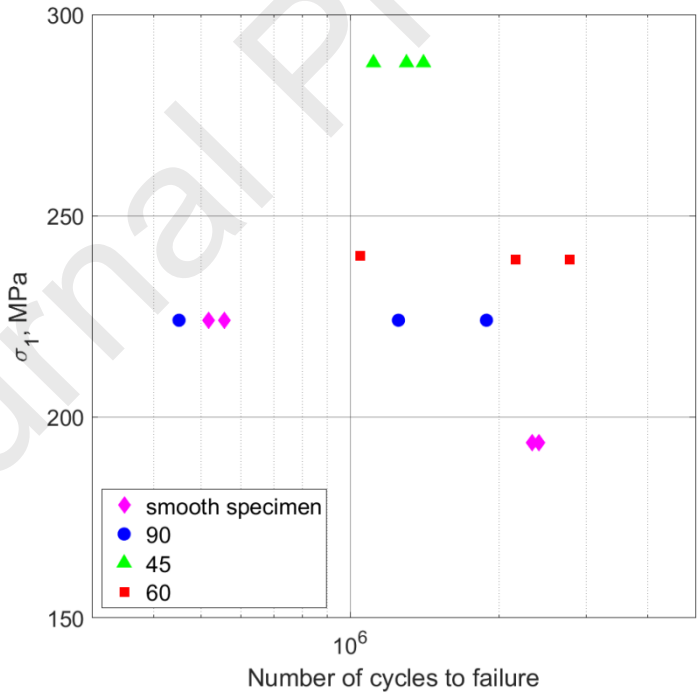

Fig. 10. S-N diagram for stresses calculated according to the different averaging criteria under torsion: (a) Huber-Mises stress $\sigma_{HM,ave}$, (b) first principal stress σ_{1_ave}.

Submitted to International Journal of Fatigue
VSI: Fatigue – ICSI2021
August 2022

NON-LOCAL VOLUMETRIC APPROACH TO ANALYSIS DEFECT'S SHAPE INFLUENCE ON SPECIMENS DURABILITY SUBJECTED TO BENDING AND TORSION

Zbigniew Marciniak[a]*, Ricardo Branco[b], Rui F. Martins[c], Wojciech Macek[d], Dariusz Rozumek[a],

[a]*Opole University of Technology, Department of Mechanics and Machine Design, Mikołajczyka 5, 45-271 Opole, Poland*

[b]*CEMMPRE, Department of Mechanical Engineering, University of Coimbra, Rua Luís Reis Santos, Pinhal de Marrocos, 3030-788 Coimbra, Portugal*

[c]*UNIDEMI, Department of Mechanical and Industrial Engineering, Nova School of Science and Technology, Universidade NOVA de Lisboa, Campus de Caparica, 2829-516 Caparica, Portugal*

[d]*Gdańsk University of Technology, Faculty of Mechanical Engineering and Ship Technology, 11/12 Gabriela Narutowicza, Gdańsk, 80-233, Poland*

* Corresponding author: z.marciniak@po.edu.pl

HIGHLIGHTS

- The non-local volumetric method was used to analyse surface-defected specimens.
- Fatigue behaviour of surface-defected specimens under bending and torsion is studied.
- Finite element analysis was performed to determine the critical volume.
- The non-local volumetric method can help engineers in advanced fatigue design.

Declaration of interests

☒ The authors declare that they have no known competing financial interests or personal relationships that could have appeared to influence the work reported in this paper.

☐The authors declare the following financial interests/personal relationships which may be considered as potential competing interests: